



UNIVERSITY OF LEEDS

This is a repository copy of *Emergence of healing in the Antarctic ozone layer*.

White Rose Research Online URL for this paper:

<http://eprints.whiterose.ac.uk/101876/>

Version: Accepted Version

Article:

Solomon, S, Ivy, DJ, Kinnison, D et al. (3 more authors) (2016) Emergence of healing in the Antarctic ozone layer. *Science*, 353 (6296). pp. 269-274. ISSN 0036-8075

<https://doi.org/10.1126/science.aae0061>

© 2016, American Association for the Advancement of Science. This is the author's version of the work. It is posted here by permission of the AAAS for personal use, not for redistribution. The definitive version was published in *Science* on 15 Jul 2016: Vol. 353, Issue 6296, DOI: 10.1126/science.aae0061.

Reuse

Unless indicated otherwise, fulltext items are protected by copyright with all rights reserved. The copyright exception in section 29 of the Copyright, Designs and Patents Act 1988 allows the making of a single copy solely for the purpose of non-commercial research or private study within the limits of fair dealing. The publisher or other rights-holder may allow further reproduction and re-use of this version - refer to the White Rose Research Online record for this item. Where records identify the publisher as the copyright holder, users can verify any specific terms of use on the publisher's website.

Takedown

If you consider content in White Rose Research Online to be in breach of UK law, please notify us by emailing eprints@whiterose.ac.uk including the URL of the record and the reason for the withdrawal request.



eprints@whiterose.ac.uk
<https://eprints.whiterose.ac.uk/>

1 **Title: Emergence of Healing in the Antarctic Ozone Layer**

2
 3 **Authors:** Susan Solomon¹, Diane J. Ivy¹, Doug Kinnison², Michael J. Mills², Ryan R. Neely
 4 III^{3,4}, Anja Schmidt³

5 **Affiliations:**

6 ¹Department of Earth, Atmospheric, and Planetary Science, Massachusetts Institute of
 7 Technology, Cambridge, Massachusetts, 02139, USA

8
 9 ²Atmospheric Chemistry Observations and Modeling Laboratory, National Center for
 10 Atmospheric Research, Boulder, PO Box 3000, Colorado, 80305, USA

11 ³School of Earth and Environment, University of Leeds, Leeds, UK

12
 13 ⁴National Centre for Atmospheric Science, University of Leeds, Leeds, UK

14 **Abstract:** Industrial chlorofluorocarbons that cause ozone depletion have been phased out under
 15 the Montreal Protocol. A chemically-driven increase in polar ozone (or “healing”) is expected in
 16 response to this historic agreement. Observations and model calculations taken together indicate
 17 that the onset of healing of Antarctic ozone loss has now emerged in September. Fingerprints of
 18 September healing since 2000 are identified through (i) increases in ozone column amounts, (ii)
 19 changes in the vertical profile of ozone concentration, and (iii) decreases in the areal extent of
 20 the ozone hole. Along with chemistry, dynamical and temperature changes contribute to the
 21 healing, but could represent feedbacks to chemistry. Volcanic eruptions episodically interfere
 22 with healing, particularly during 2015 (when a record October ozone hole occurred following the
 23 Calbuco eruption).

24 **One Sentence Summary:** Observations and model calculations jointly indicate that the
 25 Montreal Protocol is healing the Antarctic ozone hole in September, despite volcanic delays.

26
 27 Antarctic ozone depletion has been a focus of attention by scientists, policymakers and the public
 28 for three decades (1). The Antarctic “ozone hole” opens up in austral spring of each year, and is
 29 measured both by its depth (typically a loss of about half of the total integrated column amount)
 30 and its size (often more than 20 million km² in extent by October). Ozone losses have also been
 31 documented in the Arctic, and at mid-latitudes in both hemispheres (2). Concern about ozone
 32 depletion prompted a worldwide phase-out of production of anthropogenic halocarbons
 33 containing chlorine and bromine, known to be the primary source of reactive halogens
 34 responsible for the depletion (2). The ozone layer is expected to recover in response, albeit very
 35 slowly, due mainly to the long atmospheric residence time of the halocarbons responsible for the
 36 loss (2).

37
 38 Ozone recovery involves multiple stages, starting with (i) a reduced rate of decline, followed by
 39 (ii) a leveling off of the depletion, and (iii) an identifiable ozone increase that can be linked to
 40 halocarbon reductions (2,3). For simplicity, we refer to the third stage of recovery as healing.
 41 All three stages of recovery have been documented in the upper stratosphere in mid- and low-
 42 latitudes, albeit with uncertainties (2, 4, 5, 6). Some studies provide evidence for all three

43 recovery stages in ozone columns at mid-latitudes, despite dynamical variability (7). While the
44 first and second stages of Antarctic and Arctic recovery have also been well documented
45 (8,9,10), recent scientific assessment concluded that the emergence of the third stage had not
46 been established by previous studies of the polar regions (2). Further, in October of 2015 the
47 Antarctic ozone hole reached a record size (11), heightening questions about whether any signs
48 of healing can be identified in either polar region.

49

50 Controls on polar ozone

51

52 Polar ozone depletion is driven by anthropogenic chlorine and bromine chemistry linked to
53 halocarbon emissions (2,12). But ozone is not expected to heal in a monotonic fashion as
54 halocarbon concentrations decrease, due to confounding factors (such as meteorological
55 changes) that induce variability from one year to another and could influence trends (2,13,14).

56

57 The exceptionally large ozone depletion in the polar regions compared to lower latitudes
58 involves polar stratospheric cloud (PSC) particles that form under cold conditions. These clouds
59 drive heterogeneous chlorine and bromine chemistry that is sensitive to small changes in
60 temperature (and hence to meteorological variability). A related and second factor is change in
61 the transport of ozone and other chemicals by circulation or mixing changes (2). Further, some
62 PSCs, as well as aerosol particles capable of driving similar chemistry, are enhanced when
63 volcanic eruptions increase stratospheric sulfur. Significant volcanic increases in Antarctic ozone
64 depletion were documented in the early 1990s following the eruption of Mount Pinatubo in 1991,
65 and are well simulated by models (15, 16). Since about 2005, a series of smaller-magnitude
66 volcanic eruptions has increased stratospheric particle abundances (17, 18), but the impact of
67 these on polar ozone recovery has not previously been estimated.

68

69 Observations and model test cases

70

71 We examine healing using balloon ozone data from the Syowa and South Pole stations. We also
72 use total ozone column measurements from South Pole and the Solar Backscatter Ultra-Violet
73 satellite (SBUV; here we average SBUV data over the region from 63°S to the polar edge of
74 coverage). The SBUV record has been carefully calibrated and compared to suborbital data (19).
75 We also employ the Total Ozone Mapping Spectrometer/Ozone Monitoring Instrument merged
76 dataset for analysis of the horizontal area of the ozone hole (TOMS/OMI; 20). Calibrated SBUV
77 data are currently only available to 2014, while the other records are available through 2015
78 (affecting the time intervals evaluated here). Model calculations are carried out with the
79 Community Earth System Model (CESM1) Whole Atmosphere Community Climate Model
80 (WACCM), which is a fully coupled state-of-the-art interactive chemistry climate model (21).
81 We use the specified dynamics option, SD-WACCM, where meteorological fields including
82 temperature and winds are derived from observations (22, 23). The analysis fields allow the
83 time-varying temperature-dependent chemistry that is key for polar ozone depletion to be
84 simulated. The model's ability to accurately represent polar ozone chemistry has recently been
85 documented (23,24). Aerosol properties are based on the Chemistry and Climate Model
86 Intercomparison (CCMI) recommendation (25) or derived inline from a version of WACCM that
87 uses a modal aerosol sub-model (23,26). The modal sub-model calculates variations in
88 stratospheric aerosols using a database of volcanic SO₂ emissions and plume altitudes based on

89 observations (Table S1) along with non-volcanic sulfur sources (particularly OCS, anthropogenic
90 SO₂, and dimethyl sulfide). The injection heights and volcanic inputs are similar to previous
91 studies (18, 27) and the calculated aerosol distributions capture the timing of post-2005 eruptions
92 observed by several tropical, mid- and high-latitude lidars, and satellite climatologies (26).
93 Based on comparisons to lidar data for several eruptions and regions (26), our modeled post-
94 2005 total stratospheric volcanic aerosol optical depths are estimated to be accurate to within
95 ±40% (see supplement). Differences between the CCMI aerosol climatology and our calculated
96 modal aerosol model results can be large, especially in the lower stratosphere (26), and can affect
97 ozone abundances.

98 The concentrations of halogenated gases capable of depleting ozone peaked in the polar
99 stratosphere around the late 1990s due to the Montreal Protocol, and are slowly declining (2,30).
100 We analyze what role these decreases in halogens play in polar ozone trends since 2000 along
101 with other drivers of variability and change. The year 2002 displayed anomalous meteorological
102 behavior in the Antarctic (28), and it is excluded from all trend analyses throughout this paper.

103 Three different model simulations are used to examine drivers of polar ozone changes since
104 2000, using full chlorine and bromine chemistry in all cases but employing (i) observed time-
105 varying changes in temperature and winds from meteorological analyses, with calculated
106 background and volcanic stratospheric particles as well as other types of PSCs (Chem-Dyn-Vol),
107 (ii) a volcanically clean case (Vol-Clean, considering only background sources of stratospheric
108 sulfur), as well as (iii) a chemistry-only case in which annual changes in all meteorological
109 factors (including the temperatures that drive chemistry) are suppressed by repeating conditions
110 for 1999 throughout, and volcanically clean aerosols are imposed (Chem-Only). The Antarctic
111 stratosphere in austral spring of 1999 was relatively cold and was deliberately chosen for large
112 chemical ozone losses. A longer run using full chemistry and CCMI aerosols illustrates the
113 model's simulation of the onset of ozone loss since 1979. Further information on statistical
114 approaches, methods, datasets, and model are provided in the supplement.

115 Our Chem-Only simulation probably represents a conservative estimate of what may reasonably
116 be considered to be chemical effects, because it does not include radiatively-driven temperature
117 changes that are expected to occur due to changes in ozone (29) and their feedback to chemical
118 processes. Temperatures and ozone are coupled because absorption of sunlight by ozone heats
119 the stratosphere. If ozone increases due to reductions in halogens, then temperatures will
120 increase, which feeds back to the chemistry (for example, by reducing the rate of temperature-
121 dependent heterogeneous reactions that deplete ozone), further increasing ozone. Such effects
122 have not been separated here from other changes in temperature or in winds (due to dynamical
123 variability or forcings such as greenhouse gases).

124

125 Antarctic ozone trends, variability, and fingerprints of healing

126

127 Most analyses of Antarctic ozone recovery to date consider October or Sep-Oct-Nov averages (7,
128 9, 10). The historic discovery of the Antarctic ozone hole was based on observations taken in
129 October (1), and healing cannot be considered complete until the ozone hole ceases to occur in
130 that month, around mid-century (2,30). However, October need not be the month when the
131 onset of the healing process emerges. A first step in understanding whether a 'signal' of the

132 onset of healing can be identified is examining trends and their statistical significance relative to
133 the ‘noise’ of interannual variability.

134
135 October displays the deepest ozone depletion of any month in the Antarctic. However, it is
136 subject to large variability due to seasonal fluctuations in temperature and transport, as well as
137 volcanic aerosol chemistry. Figure 1 shows the time series of measured Antarctic October total
138 ozone obtained from SBUV and South Pole data along with the model calculations; Tables S2
139 and S3 provide the associated post-2000 trends and 90% confidence intervals. Figure 1 shows
140 that SD-WACCM reproduces the observed October variability from year to year when all factors
141 are considered (Chem-Dyn-Vol). However, the October total ozone trends are not yet positive
142 with 90% certainty in the data, nor in the model. In contrast, other months displaying smaller
143 depletion but reduced variability (particularly September; see Figs. 1, S1; Table S2, S3) reveal
144 positive ozone trends over 2000-2014 that are statistically significant at 90% confidence in
145 SBUV and station measurements. Arctic ozone has long been known to be more variable than
146 the Antarctic (2), and no Arctic month yet reveals a significant positive trend in either the Chem-
147 Dyn-Vol model or the SBUV observations when examined in the same manner (Table S2).

148
149 The September profile of balloon ozone trends is a key test of process understanding. Figure 2
150 shows measured balloon profile trends for the South Pole and Syowa stations for 2000-2015,
151 together with WACCM model simulations. The large ozone losses measured at Syowa as the
152 ozone hole developed from 1980-2000 are also shown for comparison. Antarctic station data
153 need to be interpreted with caution due to an observed long-term shift in the position of the
154 Antarctic vortex that affects Syowa in particular in October; South Pole is however, less
155 influenced by this effect (32). The ozonesonde datasets suggest clear increases since 2000
156 between about 100 and 50 hPa (10). The simulation employing chemistry alone with fixed
157 temperatures yields about half of the observed healing, with the remainder in this month being
158 provided by dynamics/temperature. The simulations also suggest a negative contribution (offset
159 to healing) due to volcanic enhancements of the ozone depletion chemistry between about 70 and
160 200 hPa (see Figures 4 and S2 showing similar effects in other months in this sensitive height
161 range). The comparisons to the model trend profiles in Figure 2 provide an important fingerprint
162 that the Antarctic ozone layer has begun to heal in September. This is consistent with basic
163 understanding that reductions in ozone depleting substances in the troposphere will lead to
164 healing of polar ozone that emerges over time, with lags due to the transport time from the
165 troposphere to the stratosphere along with the time required for chemically-driven trends to
166 become significant compared to dynamical and volcanic variability.

167
168 The seasonal cycle of monthly total ozone trends from the SBUV satellite is displayed in Fig. 3,
169 along with model calculations for various cases. The contributions to the modeled trends due to
170 volcanic inputs (difference between Chem-Dyn-Vol and Vol-Clean simulations), chemistry
171 alone, and dynamics/temperature (difference between Vol-Clean and Chem-Only simulations)
172 are shown in the lower panel. While it is not possible to be certain that the reasons for
173 variations obtained in the observations are identical to those in the model, the broad agreement of
174 the seasonal cycle of total trends in SBUV observations and the model calculations supports the
175 interpretation here. Less dynamical variability in September compared to October (as shown by
176 smaller error bars on the dynamics/temperature term in Figure 3, bottom panel) along with strong
177 chemical recovery make September the month when the Antarctic ozone layer displays the

178 largest amount of healing since 2000. The data suggest September increases at 90% confidence
179 of 2.5 ± 1.6 DU per year over the latitudes sampled by SBUV and 2.5 ± 1.5 DU per year from the
180 South Pole sondes. These values are consistent with the Chem-Dyn-Vol model values of 2.8 ± 1.6
181 and 1.9 ± 1.5 DU per year, respectively. Because the model simulates much of the observed
182 year-to-year variability in September total ozone well for both the South Pole and for SBUV
183 observations, confidence is enhanced that there is a significant chemical contribution to the
184 trends (Fig. 1). As a best estimate, the model results suggest that roughly half of the September
185 column healing is chemical, while half is due to dynamics/temperature though highly variable.
186 The modelled total September healing trend has been reduced by about 10% due to the chemical
187 effects of enhanced volcanic activity in the latter part of 2000-2014.

188
189 Volcanic eruptions affect polar ozone depletion because injections of sulfur enhance the surface
190 areas of liquid PSCs and aerosol particles (33). Higher latitude eruptions directly influence the
191 polar stratosphere but tropical eruptions can enhance polar aerosols following transport. The
192 model indicates that numerous moderate eruptions since about 2005 have affected polar ozone in
193 both hemispheres (see Table S1 for eruptions, dates, and latitudes), particularly at pressures from
194 about 70-300 hPa (Fig. 4). At pressures above about 100 hPa, temperatures are generally too
195 warm for many PSCs to form, but there is sufficient water that effective heterogeneous chemistry
196 can take place under cold polar conditions (12). Peak volcanic losses locally as large as 30% and
197 55% are calculated in the Antarctic in 2011 and 2015, mainly due to the Chilean eruptions of
198 Puyehue-Cordón Caulle and Calbuco, respectively; volcanic contributions to depletions tracing
199 to tropical eruptions are also obtained in several earlier years. At these pressures, contributions
200 to the total column are small but significant: the integrated additional Antarctic ozone column
201 losses averaged over the polar cap are between 5 and 13 Dobson Units following the respective
202 eruptions shown in Figure 4.

203
204 The ozone hole typically begins to open in August each year and reaches its maximum areal
205 extent in October. Decreases in the areal extent of the October hole are expected to occur in the
206 21st century as chemical destruction slows, but cannot yet be observed against interannual
207 variability, in part because of the extremely large hole in 2015 (Fig. S3). But monthly averaged
208 observations in September display shrinkage of 4.5 ± 4.1 million km² over 2000-2015 (Fig. 5, left
209 panel). The model underestimates the observed September hole size by about 15% on average,
210 but yields similar variability (Fig. 5) and trends (4.9 ± 4.7 million km²). The right panel of Figure
211 5 shows that the observed and modeled day of year when the ozone hole exceeds a threshold
212 value of 12 million km² is occurring later in recent years, indicating that early September holes
213 are becoming smaller (see Fig. 6). This result is robust to the specific choice of threshold value,
214 and implies that the hole is opening more slowly as the ozone layer heals. The Chem-Only
215 model results in Fig. 5 show that if temperatures, dynamical conditions, and volcanic inputs had
216 remained the same as 1999 until now, the September ozone hole would have shrunk by about
217 3.5 ± 0.3 million km² due to reduced chlorine and bromine, dominating the total shrinkage over
218 this period.

219
220 Volcanic eruptions caused the modeled area of the September average ozone holes to expand
221 substantially in several recent years. Our results as shown in Figure 5 (left panel) indicate that
222 much of the statistical uncertainty in the observed September trend is not random, but is due to
223 the expected chemical impacts of these geophysical events. In 2006, 2007, and 2008, model

224 calculations suggest that the September ozone holes were volcanically enhanced by about 1
225 million km². The size of the September ozone holes of 2011 and 2015 are estimated to have
226 been, respectively, about 1.0 million km² and 4.4 million km² larger due to volcanoes (especially
227 Puyehue-Cordón Caulle in 2011 and Calbuco in 2015) than they would otherwise have been,
228 substantially offsetting the chemical healing in those years.

229
230 Figure 6 shows that the bulk of the seasonal growth of the ozone hole typically occurs between
231 about days 230 and 250 (late August to early September). As the ozone layer heals, the growth
232 of the hole is expected to occur later in the year (middle and bottom panels), in agreement with
233 observations (top). The slower rates of early season growth are key to the trend of shrinkage of
234 the September averaged ozone hole. For example, the rate of ozone loss depends strongly upon
235 the ClO concentration, so that reduced chlorine concentrations imply slower rates of ozone loss
236 after polar sunrise. The ozone hole of 2015 was considerably larger than ever previously
237 observed over several weeks in October of 2015 (but notably, not in September), and this
238 behavior is well reproduced in our model only when the eruption of Calbuco is considered (Fig.
239 S3 and S4). The record-large monthly averaged ozone hole in October 2015 measured 25.3
240 million km², which was 4.8 million km² larger than the previous record year (20.6 million km² in
241 2011). When volcanic aerosols are included in the Chem-Dyn-Vol simulation, our calculated
242 monthly averaged October 2015 ozone hole is 24.6 million km², while the corresponding value
243 in the volcanically clean simulation is much smaller, 21.1 million km² (Figure S3). Therefore,
244 our calculations indicate that cold temperatures and dynamics alone made a much smaller
245 contribution to establishing the October 2015 record than the volcanic aerosols (see Fig. S3, S4),
246 and the cold temperatures are expected to be at least partly a feedback to the volcanically-
247 enhanced large ozone losses. Further, the conclusion that the volcanic aerosols were the
248 dominant cause of the record size of the October 2015 ozone hole would hold based on our
249 calculations even if the volcanic aerosol amounts were overestimated by a factor of several (a
250 much larger error than indicated by our comparison of the model to lidar data for multiple
251 eruptions in 26, see supplement).

252
253 The reason or reasons for the dynamics/temperature contributions to healing of the Antarctic
254 ozone layer are not clear. The dynamical/temperature contributions to healing estimated in Fig. 3
255 vary by month in a manner that mirrors the ozone depletion in spring, suggesting linkages to the
256 seasonality of the depletion itself and hence possible dynamical feedbacks. Some models (31,
257 34, 35) suggest that a reduction in transport of ozone to the Antarctic occurred as depletion
258 developed in the 1980s and 1990s, which would imply a reversal and hence enhanced healing as
259 ozone rebounds. But others indicate that ozone depletion increased the strength of the
260 stratospheric overturning circulation (36); and a reversal of this factor during recovery would
261 impede healing. While there is robust agreement across models that climate change linked to
262 increasing greenhouse gases should act to increase the strength of the stratospheric overturning
263 circulation, observations show mixed results (37); further, the seasonality has not been
264 established, and the magnitude in the Antarctic is uncertain. Internal variability of the climate
265 system linked for example to variations in El Niño could also affect the trends.

266
267
268
269

270 Conclusion

271
272 After accounting for dynamics/temperature and volcanic factors, the fingerprints presented here
273 indicate that healing of the Antarctic ozone hole is emerging. Our results underscore the
274 combined value of balloon and satellite ozone data, as well as volcanic aerosol measurements
275 together with chemistry-climate models to document the progress of the Montreal Protocol in
276 recovery of the ozone layer.

277 References and Notes

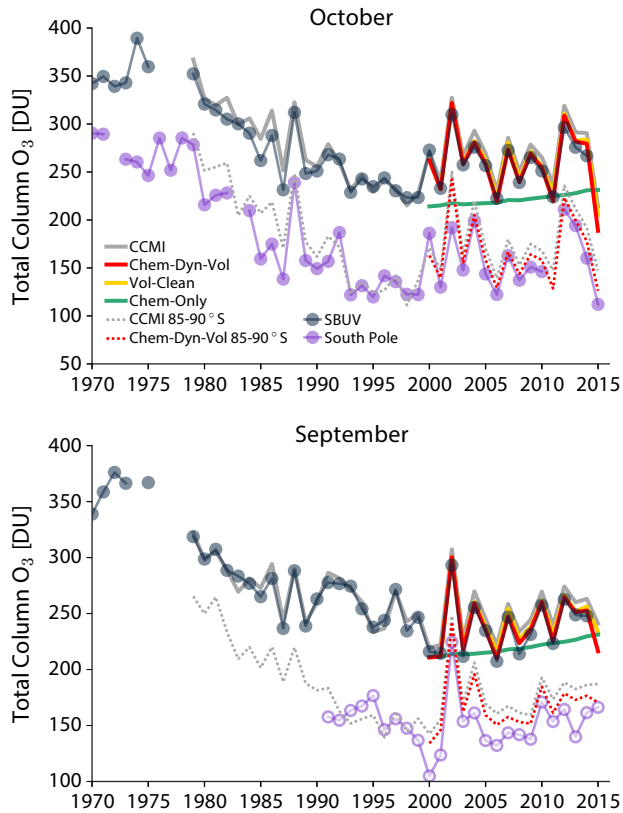
- 278 1. J. C. Farman, B. G. Gardiner, J. D. Shanklin, Large losses of total ozone in Antarctica reveal
279 seasonal ClO_x/NO_x interaction. *Nature* **315**, 207–210 (1985).
- 280 2. WMO/UNEP (World Meteorological Organization/United Nations Environment Programme):
281 Scientific Assessment of Ozone Depletion, Global Ozone Research and Monitoring Project
282 (Report No. 55, 416 pp., Geneva, Switzerland, 2014).
- 283 3. D. J. Hofmann, S. J. Oltmans, J. M. Harris, B. J. Johnson, J. A. Lathrop, Ten years of
284 ozonesonde measurements at the south pole: implications for recovery of springtime Antarctic
285 ozone. *J. Geophys. Res.* **102**, 8931-8943 (1997).
- 286 4. M. J. Newchurch et al., Evidence for slowdown in stratospheric ozone loss: First stage of
287 ozone recovery. *J. Geophys. Res.* **108**, 4507, doi:10.1029/2003JD003471 (2003).
- 288 5. N. R. P. Harris et al., Past changes in the vertical distribution of ozone – Part 3: Analysis and
289 interpretation of trends. *Atmos. Chem. Phys.* **15**, 9965–9982 (2015).
- 290 6. F. Tummon et al., Intercomparison of vertically resolved merged satellite ozone data sets:
291 interannual variability and long-term trends. *Atmos. Chem. Phys.* **15**, 3021–3043 (2015).
- 292 7. T. G. Shepherd et al., Reconciliation of halogen-induced ozone loss with the total column
293 ozone record. *Nat. Geo.* **7**, 443-449 (2015).
- 294 8. E.-S. Yang et al., First stage of Antarctic ozone recovery. *J. Geophys. Res.* **113**, D20308,
295 10.1029/2007JD009675, (2008).
- 296 9. M. L. Salby, E. Titova, L. Deschamps, Rebound of Antarctic ozone. *Geophys. Res. Lett.* **38**,
297 L09702, doi:10.1029/2011GL047266 (2011).
- 298 10. J. Kuttippurath et al., Antarctic ozone loss in 1979-2010: first sign of ozone recovery. *Atmos.*
299 *Chem. Phys.* **13**, 1625–1635 (2013).
- 300 11. See <https://www.wmo.int/pages/prog/arep/WMOAntarcticOzoneBulletins2015.html>,
301 published by the World Meteorological Organization.
- 302 12. S. Solomon, Stratospheric ozone depletion: a review of concepts and history. *Rev. Geophys.*
303 **37**, 275–316 (1999).
- 304 13. J. Kuttippurath et al., Variability in Antarctic ozone loss in the last decade (2004–2013): high-
305 resolution simulations compared to Aura MLS observations. *Atmos. Chem. Phys.* **15**, 10385–

- 306 10397 (2015).
- 307 14. N. J. Livesey, M. L. Santee, G.L. Manney, A Match-based approach to the estimation of
308 polar stratospheric ozone loss using Aura Microwave Limb Sounder observations. *Atm. Chem.*
309 *Phys.* **15**, 9945-9963 (2015).
- 310 15. D. J. Hofmann, S. J. Oltmans, Antarctic ozone during 1992: evidence for Pinatubo volcanic
311 aerosol effects. *J. Geophys. Res.* **98**, 18555-18561 (1993).
- 312 16. R. W. Portmann et al., Role of aerosol variations in anthropogenic ozone depletion in the
313 polar regions. *J. Geophys. Res.* **101**, 22991–23006 (1996).
- 314 17. J.-P. Vernier, et al., Major influence of tropical volcanic eruptions on the stratospheric
315 aerosol layer during the last decade. *Geophys. Res. Lett.* **38**(12), L12807,
316 doi:10.1029/2011GL047563 (2011).
- 317 18. C. J. Bruehl, C. J. Lelieveld, H. Tost, M. Hoepfner, N. Glatthor, Stratospheric sulfur and its
318 implications for radiative forcing simulated by the chemistry climate model EMAC. *J. Geophys.*
319 *Res. Atmos.* **120**, 2103–2118 (2015).
- 320 19. R. D. McPeters, P. K. Bhartia, D. Haffner, G. L. Labow, L. Flynn, The version 8.6 SBUV
321 ozone data record: an overview. *J. Geophys. Res.* **118**, 8032–8039 (2013).
- 322 20. W. Chehade, M. Weber, J. P. Burrows, Total ozone trends and variability during 1979-2012
323 from merged data sets of various satellites. *Atmos. Chem. Phys.* **14**, 7059–7074 (2014).
- 324 21. D. R. Marsh et al., Climate Change from 1850 to 2005 Simulated in CESM1(WACCM). *J.*
325 *Clim.* **26**, 7372–7391 (2013).
- 326 22. A. Kunz, L. L. Pan, P. Konopka, D. E. Kinnison, S. Tilmes, Chemical and dynamical
327 discontinuity at the extratropical tropopause based on START08 and WACCM analyses. *J*
328 *Geophys. Res.* **116**(D24), D24302, doi:10.1029/2011JD016686 (2011).
- 329 23. See materials and methods in the supplement, available at the Science Web site.
- 330 24. S. Solomon, D. Kinnison, J. Bandoro, R. R. Garcia, Polar ozone depletion: An update. *J.*
331 *Geophys. Res.* **120**, doi:10.1002/ 2015JD023365 (2015).
- 332 25. F. Arfeuille, et al., Modeling the stratospheric warming following the Mt. Pinatubo eruption:
333 uncertainties in aerosol extinction. *Atmos. Chem. Phys.* **13**, 11221–11234 (2013).
- 334 26. M. J. Mills, et al., Global volcanic aerosol properties derived from emissions, 1990-2014,
335 using WACCM5. *J. Geophys. Res.* **121**, 2332-2348 (2015).
- 336 27. M. Hoepfner et al., Sulfur dioxide (SO₂) from MIPAS in the upper troposphere and lower
337 stratosphere 2002–2012. *Atm. Chem. Phys.* **15**, 7017-7037 (2015).
- 338 28. A. A. Scaife, et al., Stratospheric vacillations and the major warming over Antarctica in

- 339 2002. *J. Atm. Sci.* **62**, 629-639 (2005).
- 340 29. P. M. Forster, R. S. Freckleton, K. P. Shine, On aspects of the concept of radiative forcing.
341 *Clim. Dyn.* **13**, 547-560 (1997).
- 342 30. P. A. Newman, E. R. Nash, S. R. Kawa, S. A. Montzka, S. M. Schauffler, When will the
343 Antarctic ozone hole recover? *Geophys. Res. Lett.* **33**, L12814, doi:10.1029/2005GL025232
344 (2006).
- 345 31. S. Muel, S. Oberlaender-Hayn, J. Abalichin, U. Langematz, Nonlinear response of modeled
346 stratospheric ozone to changes in greenhouse gases and ozone depleting substances in the recent
347 past. *Atm. Chem. Phys.* **15**, 6897-6911, doi:10.5194/acp-15-6897-2015, (2015).
- 348 32. B. Hassler, G. E. Bodeker, S. Solomon, P. J. Young, Changes in the polar vortex: Effects on
349 Antarctic total ozone observations at various stations. *Geophys. Res. Lett.* **38**, L01805,
350 doi:10.1029/2010GL045542 (2011).
- 351 33. A. Tabazadeh, K. Drdla, M. R. Schoeberl, P. Hamill, O. B. Toon, Arctic “ozone hole” in a
352 cold volcanic stratosphere. *PNAS* **99**, 2609-2612 (2002).
- 353 34. P. Braesicke, et al., Circulation anomalies in the Southern Hemisphere and ozone changes.
354 *Atmos. Chem. Phys.* **13**, 10677–10688 (2013).
- 355 35. F. Li, J. Austin, J. Wilson, The strength of the Brewer–Dobson circulation in a changing
356 climate: coupled chemistry–climate model simulations. *J. Clim.* **21**, 40-57 (2008).
- 357 36. C. McLandress, T. G. Shepherd, Simulated anthropogenic changes in the Brewer–Dobson
358 Circulation, including its extension to high latitudes. *J. Clim.* **22**, 1516-1540 (2009).
- 359 37. N. Butchart, The Brewer-Dobson circulation. *Rev. Geophys.* **52**, 157–184 (2014).

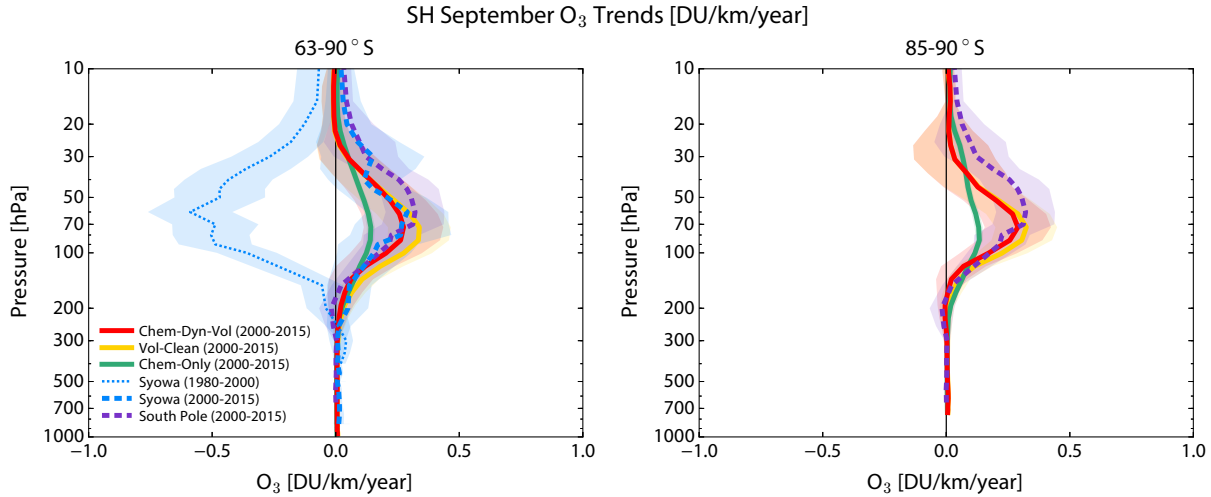
360 **Acknowledgments:** We thank Simone Tilmes (NCAR) for help with the MERRA data. DEK
361 and SS were partially supported by NSF FESD grant OCE-1338814 and DI was supported by
362 NSF atmospheric chemistry division grant 1539972. AS was supported by an Academic
363 Research Fellowship from the University of Leeds, an NCAR visiting scientist grant and NERC
364 grant NE/N006038/1. The National Center for Atmospheric Research (NCAR) is sponsored by
365 the U.S. National Science Foundation. WACCM is a component of the Community Earth System
366 Model (CESM), which is supported by the National Science Foundation (NSF) and the Office of
367 Science of the U.S. Department of Energy. We are grateful to David Fahey, Birgit Hassler,
368 William Dean McKenna, and the anonymous reviewers for helpful comments. Instructions for
369 access to data reported in this paper are given in the supplement.

370

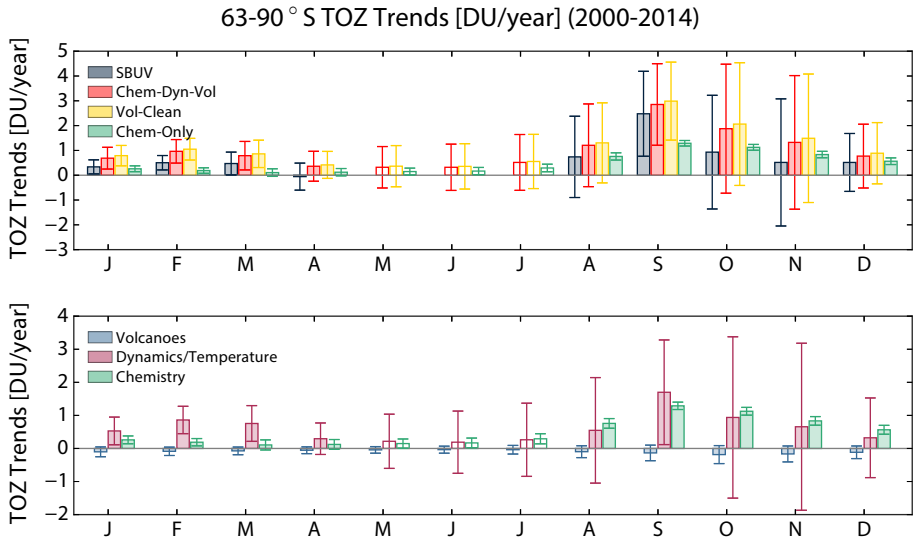


371
 372
 373
 374
 375
 376
 377
 378
 379
 380
 381

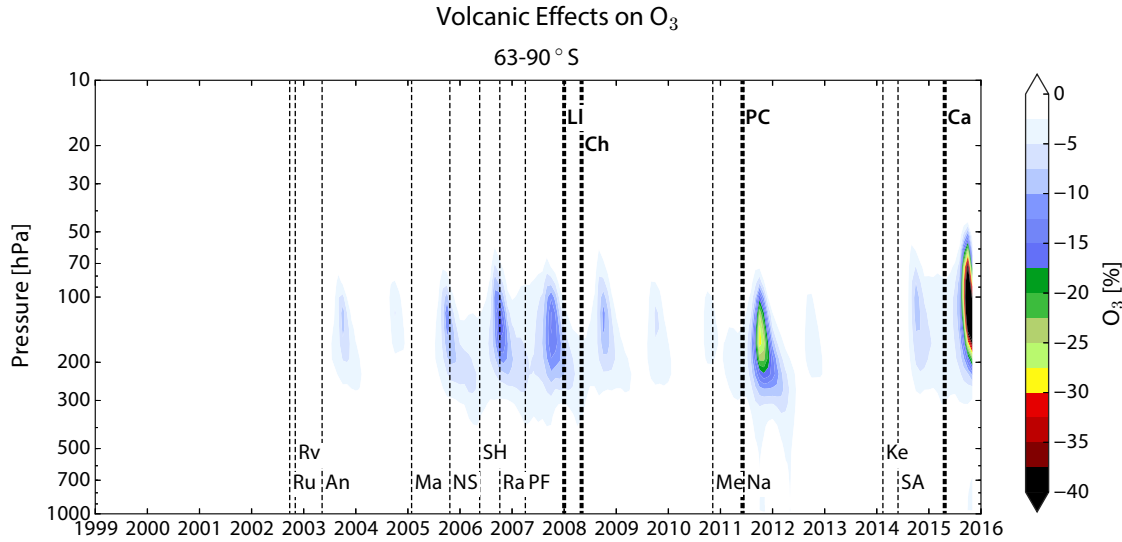
Fig. 1. Monthly averaged Antarctic total ozone column for October and September, from SBUV and South Pole observations and for a series of model calculations. Total ozone data at the geographic South Pole are from Dobson observations where available (filled circles) and balloon sondes (open circles, for September, when there is not sufficient sunlight for the Dobson). SBUV data for each month are compared to model runs averaged over the polar cap latitude band accessible by the instrument, while South Pole data are compared to simulations for 85-90°S.



382
 383 Fig. 2. Trends in September ozone profiles from balloons at Syowa (69°S, 39.58°E, left panel)
 384 and South Pole (right panel) stations versus pressure, along with model simulations averaged
 385 over the polar cap for the Chem-Dyn-Vol, Vol-Clean, and Chem-Only model simulations. The
 386 shading represents the uncertainties on the trends at the 90% statistical confidence interval.
 387

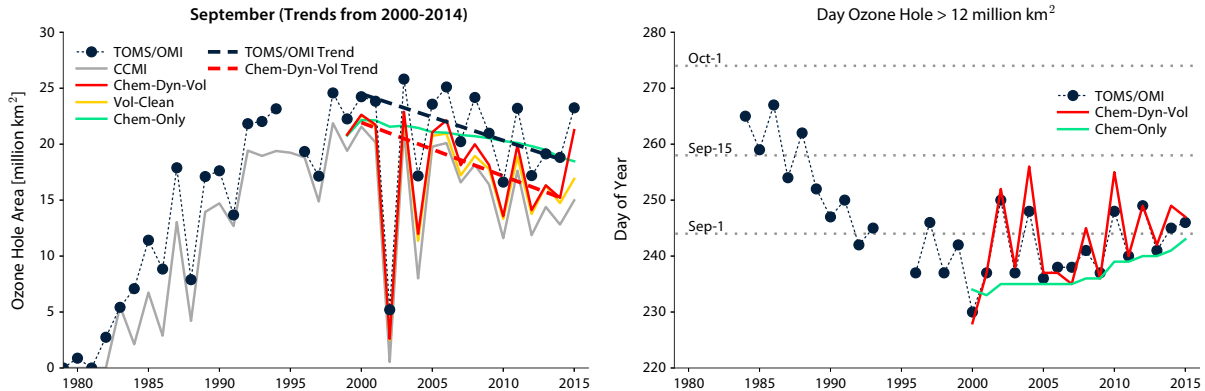


388
 389
 390
 391 Fig. 3. (top) Trends in total ozone abundance (TOZ) from 2000-2014 by month, from monthly
 392 and polar cap averaged SBUV satellite observations together with numerical model simulations
 393 masked to the satellite coverage, for the Chem-Dyn-Vol, Vol-Clean, and Chem-Only
 394 simulations; error bars denote 90% statistical confidence intervals. (bottom) Contributions to
 395 the simulated monthly trends in total ozone abundance driven by dynamics/temperature (from
 396 Vol-Clean minus Chem-Only), chemistry only, and volcanoes (from Chem-Dyn-Vol minus Vol-
 397 Clean). In austral winter, SBUV measurements do not extend to 63°S, therefore the model
 398 averages for those months cover 63-90°S (open bars).



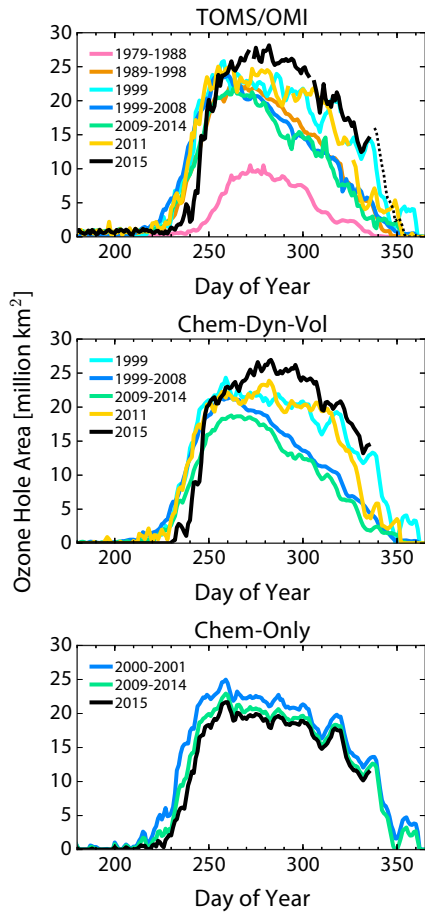
399
 400 Fig. 4. Model calculated percentage changes in local concentrations of ozone due to a series of
 401 moderate volcanic eruptions (from Dyn-Chem-Volc minus Vol-Clean simulations), averaged
 402 over the Antarctic polar cap as a function of pressure and month. Volcanic eruptions that have
 403 dominated the changes are indicated, with tropical eruptions at the bottom while higher latitude
 404 eruptions are shown at the top, where An=Anatahan, Ca=Calbuco, Ch=Chaiten, Ke=Kelut,
 405 Ll=Llaima, Ma=Manam, Me=Merapi, Na=Nabro, NS=Negra Sierra, PC= Puyehue-Cordón
 406 Caulle, PF= Piton de la Fournaise, Ra=Rabaul (also referred to as Tauruvur), Ru=Ruang,
 407 Rv=Reventador, SA=Sangeang Api, SH=Soufriere Hills.

408



409
 410 Fig. 5. Annual size of the September monthly average ozone hole (defined as the region where
 411 total ozone amount is less than 220 DU, left panel) from TOMS satellite observations together
 412 with numerical model simulations for the Chem-Dyn-Vol, Vol-Clean, and Chem-Only
 413 simulations. Trends in the TOMS observations (heavy dashed black line) and the Chem-Dyn-
 414 Vol model calculations from 2000-2015 (heavy dashed red line) are also indicated. The annual
 415 day of year when the size of the ozone hole exceeds 12 million km² (and remains above that
 416 value for at least 3 days) in the TOMS observations and model simulations are shown in the right
 417 panel.

418



419
 420 Fig. 6. Daily measurements (top) and model calculations (middle and bottom) of the size of the
 421 Antarctic ozone hole versus day of year in different time intervals or years, with 2015 shown in
 422 black. Dashed black line in the top panel denotes the 2015 TOMS data after the period covered
 423 by the model runs.
 424
 425